Available online at www.sciencedirect.com
SCIENCE DIRECT®
Journal of Theoretical Biology 237 (2005) 302–315
Journal of Theoretical Biology
www.elsevier.com/locate/yjtbi

Modeling polio as a disease of development

Svetlana Bunimovich-Mendrazitsky, Lewi Stone*

Biomathematics Unit, Department of Zoology, Tel-Aviv University, Ramat Aviv 69978, Israel

Received 14 July 2004; received in revised form 21 April 2005; accepted 22 April 2005
Available online 21 June 2005

Abstract

Poliomyelitis is a disease which began to appear in epidemic proportions in the late 19th century, paradoxically, just at the time when living conditions and developments in health were transforming enormously for the better. We present a simple age-class model that explains this "disease of development" as a threshold phenomenon. Epidemics arise when improved conditions in hygiene are able to reduce disease transmission of polio amongst children below a critical threshold level. This generates a large susceptible adult population in which, under appropriate conditions, epidemics can propagate. The polio model is analysed in terms of its bifurcation properties and in terms of its non-equilibrium outbreak dynamics.

Keywords: Disease of development; Polio; Age-structured model; Threshold; Contact rate; Environmental factor; Epidemic

1. Introduction

"Poliomyelitis" is an epidemiological disease that has accompanied humankind throughout history. The earliest identifiable reference to paralytic poliomyelitis is an Egyptian stone engraving that dates back to more than 3500 years ago, and depicts a crippled young man, apparently a priest, with all the characteristic features of polio (Paul, 1971). The name itself is derived from the Greek words "polios", or grey (referring to the grey matter of the nervous system) and "myelos" for marrow (referring to the myelin sheath membrane that surrounds the spinal cord) (Thomas and Robbins, 1997). Polio is also a prominent example of what is now referred to as a disease of development (Miller and Gay, 1997; Krause, 1998; Sutter et al., 1999). This is because in the late 19th and early 20th centuries, during a period of intense industrial development, social revolution and increased hygiene, there was a large increase of poliomyelitis with epidemics of a scale never seen previously (Figs. 1 and 2).

Poliomyelitis is caused by poliovirus, which invades local lymphoid tissue and enters the blood stream. Poliovirus enters through the mouth, attaches to receptors on the epithelium of the throat and intestine, and replicates inside these cells. Polioviruses are spread directly or indirectly from person to person by droplets or aerosols and by fecal contamination of hands, eating utensils, milk, food and water (Dowdle and Birmingham, 1997). Exposure to poliomyelitis results in one of the following consequences: inapparent infection without symptoms (72% of people), minor illness (24%), non-paralytical poliomyelitis (4%) or paralytic poliomyelitis (<1%) (Sutter et al., 1999). Paralytic poliomyelitis is a severe form of the disease which occurs when a systemic infection moves to the central nervous system (CNS) and destroys neuronal cells. Although the paralytic form is an infrequent manifestation of polio, obviously a large-scale outbreak of the disease with tens of thousands of polio cases, can give rise to a large number of paralytic cases.

There is no simple all-encompassing theory that is capable of explaining the history and dynamics of polio epidemics. The best known theory is based on the somewhat controversial observation that the ratio of

*Corresponding author. Tel.: +972 3 6409806; fax: +972 3 6409403.
E-mail address: lew521@yahoo.com (L. Stone).

0022-5193/$ - see front matter © 2005 Elsevier Ltd. All rights reserved.
doi:10.1016/j.jtbi.2005.04.017

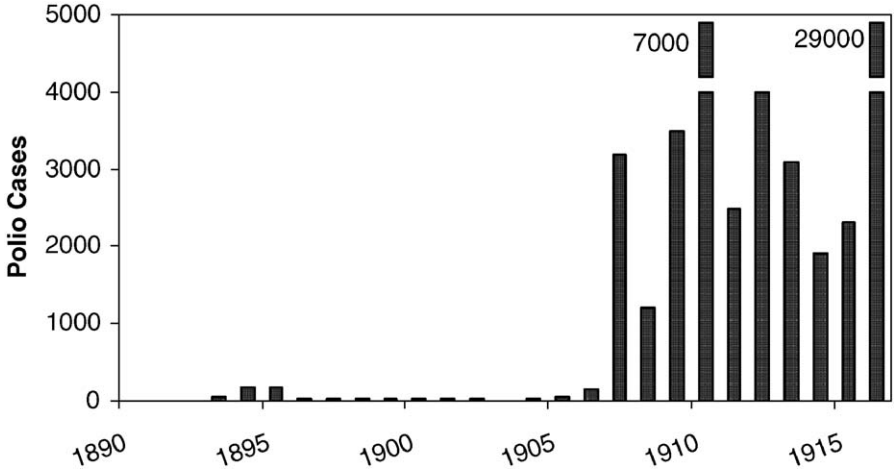

Fig. 1. Number of reported polio incidence cases (mainly paralytic) per year in United State from 1890 to 1916 (adapted from Nathanson and Martin, 1979).

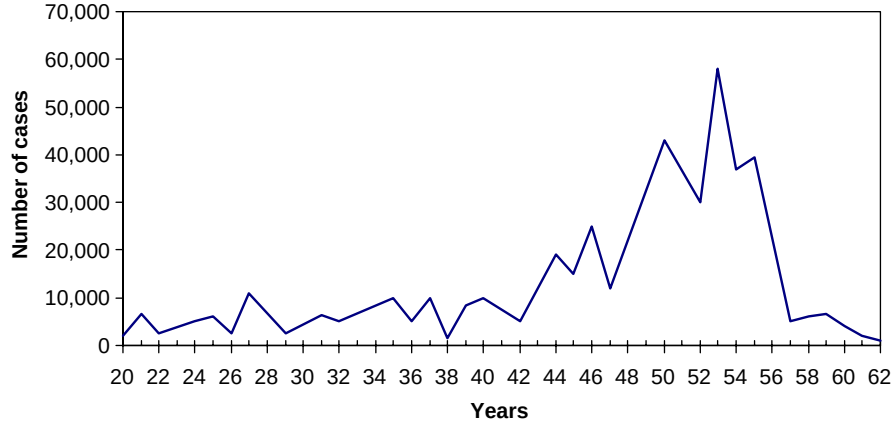

Fig. 2. Number of reported polio incidence cases (mainly paralytic) per year in United State from 1920 to 1962 (adapted from Sutter et al., 1999).

paralytic cases to the total number of infectives (case:-infection ratio) increases with age (Nathanson and Martin, 1979; Miller and Gay, 1997). Thus age tends to increase the dangers of poliomyelitis, with adults more likely to be paralyzed or killed by the virus than children. Before the developments associated with the 20th century, almost all children were exposed to poliovirus during infancy, largely due to poor sanitation conditions. Sewage entered watersheds without treatment transporting the polio virus into rivers, lakes, streams and thus direct into the water supplies. Indirectly, polio virus passed through the food chain and could be traced even in milk supplies. Due to the low case:infection ratio of infants, and due to protection from transplacentally acquired maternal antibodies, paralysis was rare amongst young children, although the disease itself was endemic. Because of their exposure to polio at an early age, infected infants acquired immunity to the disease thereby protecting them in later life.

The transformation of poliomyelitis from endemic to epidemic occurred, paradoxically, just at the time of major hygienic improvements in the late 19th century. This period saw developments in technologies such as waste disposal, widespread use of indoor plumbing, and careful separation of sewage from drinking water. Improvements in sanitation reduced the transmissibility of the disease. As such, children were no longer exposed to the polio virus at an early age, and thus remained susceptible to the disease as older children or even adults. The average age of first-infection in the United States population was less than 5 years in mid 19th century to early 20th century (Sutter et al., 1999), and is likely to have been under 2 years of age similar to the situation in many developing countries (Sutter et al., 1999; Melnick, 1994). By the 1940s the average age increased to 9 years (Sutter et al., 1999). The increase in the average age of infection led to a large and growing pool of older unprotected susceptible individuals—the perfect setting for epidemics to ignite. As the

case:infection ratio is larger in higher age brackets of the population (no longer protected by maternal antibodies), this further increased incidences of paralytic polio.

In the late 19th century and early 20th century, epidemics occurred in industrial countries, such as Sweden, Norway, and the United States. The three largest poliomyelitis outbreaks of that period occurred in Vermont in 1894 (132 cases), Sweden in 1905 (1031 cases) and New York in 1916 (9000 cases). Fig. 1 illustrates the sudden increased number of paralytic poliomyelitis cases at the beginning of 20th century in the United States. The incidence of polio rose steadily in the 1940s in developed nations peaking in the 1950s (Fig. 2). The worst recorded polio epidemic in US occurred in 1952 with 57 628 cases reported (Sutter et al., 1999). Two factors are considered responsible for this large-scale epidemic. Firstly, during Word War II, 50 million soldiers worldwide left their homes to be sent overseas. Many of these soldiers, nearly all susceptible to polio, traveled to developing countries where polio was endemic (Paul, 1971; Krause, 1998). Western soldiers became victims of domestic sanitary conditions and subsequently developed paralytic poliomyelitis. Secondly, at the same time, the western population increased drastically due to a post-war baby boom, thus creating an increased pool of susceptibles. Finally, that paralytic poliomyelitis became more prominent in developed countries is made clear in Fig. 3. Keeping in mind that developing countries are associated with higher infant mortality rates, the graph shows that countries with lower mortality rates generally have higher numbers of polio cases (per million population).

Although there have been numerous attempts at modeling the population dynamics of poliomyelitis (Hillis, 1979; Cvjetanovic et al., 1982; Anderson and May, 1991; Ranta et al., 2001), to our knowledge no model has successfully explained the effect seen in Figs. 1 and 2 as a threshold phenomenon, as is attempted here. An interesting model of Coleman et al. (2001) shows that endemic infection rates can paradoxically increase with increasing disease control measures (analogous to sanitation here) as a result of the population's age structure. However, Coleman et al. (2001) do not attempt to explain the non-equilibrium outbreak dynamics. Our goal is to build a model taking into consideration previous theories, to explain these sudden and dramatic peaks in paralytic cases.

2. Two class age-structured epidemic model

We use the classical age-structured mathematical model of Schenzle (1984) as a framework for studying "diseases of development", with poliomyelitis taken as a particular case-study. The model considers a constant population having a fixed number of host individuals N, each belonging to only one of four different possible groups: susceptible (S), exposed (E), infected (I) and recovered (R). When exposed to the infection, susceptible individuals are transferred to the exposed group and remain for a latent period of 3–6 days (Sutter et al., 1999) after which they pass directly to the infectious group. Infected individuals here include those with minor and major illness, as well as paralytic poliomyelitis, and the infectious period can last as long as 20 days (WHO, 1993). Upon recovery from the infection, individuals join the recovered group. The transfer between the different groups may be notated in the following short form:

$$S \to E \to I \to R.$$

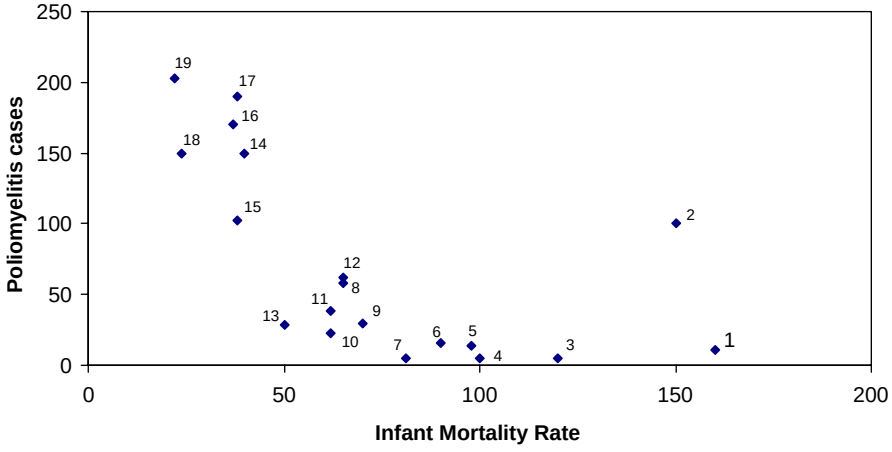

Fig. 3. A comparison of infant mortality rates and the incidence of paralytic poliomyelitis in different countries in the beginning of 1950s (adapted from Paul, 1971). Horizontal axis gives infant mortality per 1.000 live births. Vertical axis gives poliomyelitis cases per million of the population. Countries are assigned the following numbers: (1) Egypt; (2) Chile; (3) Algeria; (4) Yugoslavia; (5) Mexico; (6) Portugal; (7) Colombia; (8) Italy; (9) Argentina; (10) Spain; (11) France; (12) Germany; (13) Uruguay; (14) Canada; (15) England and Wales; (16) Denmark; (17) USA; (18) Australia; (19) Sweden.

To simplify the modeling task, we assume that the exposed group has little impact on the dynamics due to the relatively short incubation period of the disease (3–6 days) and can be ignored. In the case of polio, the exposed period is particularly short because the virus is often found in the pharynx and/or the stool whereupon an exposed individual may immediately infect other people.

The population is crudely divided into two age classes, children and adults, and the different epidemic scenarios associated with "diseases of development" are attributed to the interactions between these classes. Individuals below 2 years of age belong to the "children's" age-class, while individuals above 2 years of age are defined as the "adult"-class. The division was chosen because, as discussed earlier, the average age of poliovirus infection was likely to be 2 years in the more developed countries in the late 1800's and also a good reflection of that found in many developing countries (Sutter et al., 1999; Melnick, 1994). Note that the exact age itself is to some extent arbitrary—the main goal is to divide the population into two reasonably representative age classes.

Extending the notation to include two age classes, we let S_c, I_c, R_c, and S_a, I_a, R_a represent the susceptible, infective and recovered groups for children and adults, respectively. The full model may be written as follows:

$$\begin{aligned}
\frac{dS_c}{dt} &= \mu N - \left(\alpha + \mu + \frac{\beta_{cc}}{N_c} I_c + \frac{\beta_{ca}}{N_c} I_a\right) S_c,\\
\frac{dS_a}{dt} &= \alpha S_c - \left(\mu + \frac{\beta_{aa}}{N_a} I_a + \frac{\beta_{ac}}{N_a} I_c\right) S_a,\\
\frac{dI_c}{dt} &= \left(\frac{\beta_{cc}}{N_c} I_c + \frac{\beta_{ca}}{N_c} I_a\right) S_c - (\gamma_c + \alpha + \mu) I_c,\\
\frac{dI_a}{dt} &= \left(\frac{\beta_{ac}}{N_a} I_c + \frac{\beta_{aa}}{N_a} I_a\right) S_a - (\gamma_a + \mu) I_a + \alpha I_c,\\
\frac{dR_c}{dt} &= \gamma_c I_c - \mu R_c - \alpha R_c,\\
\frac{dR_a}{dt} &= \gamma_a I_a - \mu R_a + \alpha R_c. \qquad (1)
\end{aligned}$$

The structure of the model (see Fig. 4) and its parameters were decided upon as follows. Firstly, the populations birth and mortality rates are taken to be the same and set at $\mu = \frac{1}{50} = 0.02$ (year^{-1}), based on the fact that the average lifespan at the beginning of the 20th century was approximately 50 years. As it takes 2 years from birth to pass from the children's age class to the adult age class, the transition rate is set as $\alpha = \frac{1}{2} = 0.5$. The infective periods[1] of children and adults are 10 and 20 days, respectively, which leads to recovery rates of $\gamma_c = 36 (= 360/10)$ for children and $\gamma_a = 18$ for adults. Note that since the disease duration (average $\approx$10–20 days) is relatively small compared to the transition time from the child to adult age-class (2 years), the ageing parameter α appearing in the transition from the infective class I_c to I_a may for all practical purposes be neglected.

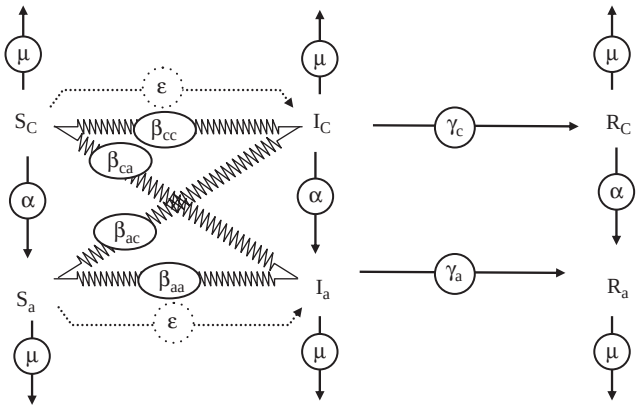

Fig. 4. Schematical view of transition between disease stages (see text).

Susceptible children and adults become infected through the usual contact process at rates governed by the random mixing between the different classes. For a multiple age class system, it is usual to let β_{ij} be the number of susceptible contacts in age-class-i, which become infected due to direct disease transmission from an infective in age-class-j. One may think of β_{ij} as $\beta_{ij} = c_j p_{ij}$, where p_{ij} is the probability of an infection being transmitted from age-class-j to a susceptible in age-class-i, and c_j is the number of contacts made by members of group-j. Following Jacquez et al. (1995), we note that infectives in age class-j make $\beta_{ij} I_j$ contacts with members of class-i that lead to infections. Of all these infective contacts, $\beta_{ij} I_j S_i / N_i$ are made with susceptibles in class-i. In our particular case, the rate of susceptible children becoming infected can be found by summing over the two classes to obtain

$$\frac{S_c}{N_c}(\beta_{cc} I_c + \beta_{ca} I_a).$$

Likewise the rate of susceptible adults becoming infected is

$$\frac{S_a}{N_a}(\beta_{aa} I_a + \beta_{ac} I_c).$$

These last terms explain the transmission rates appearing in Eq. (1).

It is useful to define:

$$N_c = S_c + I_c + R_c,$$
$$N_a = S_a + I_a + R_a,$$

[1]The infection of children is associated with minor illness which lasts 8–10 days (WHO, 1993) and is nonparalytical and often inapparent. Minor illness is often absent for adolescent and adult cases of poliomyelitis (Sutter et al., 1999) and the major illness is approximately 20 days (WHO, 1993).

which are the total numbers of children and adults in the full population. As the birth and death rates (μ) are set equal, summing all six equations in Eq. (1) retrieves the relation that the total population $N = N_c + N_a$ has zero growth rate $dN/dt = 0$, implying that for all time:

$N = \text{constant}.$

As such, the last equation in Eq. (1) is taken to be redundant since R_a can always be obtained through the equation:

$$R_a = N - S_c - I_c - R_c - S_a - I_a.$$

We thus need only examine a system of five nonlinear first-order differential equations.

Eq. (1) may be normalized by taking all variables as fixed proportions of the population N, and introducing the dashed variables:

$$S_c' = \frac{S_c}{N}, \quad I_c' = \frac{I_c}{N}, \quad R_c' = \frac{R_c}{N}, \quad S_a' = \frac{S_c}{N},$$
$$I_a' = \frac{I_a}{N}, \quad R_a' = \frac{R_a}{N}, \quad N_c' = \frac{N_c}{N}, \quad N_a' = \frac{N_a}{N}. \tag{2}$$

Rewriting the equations in these new variables (2) and dropping dashes gives:

$$\frac{dS_c}{dt} = \mu - \left(\alpha + \mu + \frac{\beta_{cc}}{N_{cc}} I_c + \frac{\beta_{ca}}{N_c} I_a\right) S_c,$$
$$\frac{dS_a}{dt} = \alpha S_c - \left(\mu + \frac{\beta_{aa}}{N_a} I_a + \frac{\beta_{ac}}{N_a} I_c\right) S_a,$$
$$\frac{dI_c}{dt} = \left(\frac{\beta_{cc}}{N_c} I_c + \frac{\beta_{ca}}{N_c} I_a\right) S_c - (\gamma_c + \mu) I_c,$$
$$\frac{dI_a}{dt} = \left(\frac{\beta_{ac}}{N_a} I_c + \frac{\beta_{aa}}{N_a} I_a\right) S_a - (\gamma_a + \mu) I_a,$$
$$\frac{dR_c}{dt} = \gamma_c I_c - (\alpha + \mu) R_c. \tag{3}$$

with

$$N = N_c + N_a = 1.$$

The models' equilibria are found by setting all rates of Eq. (3) to zero and solving the resulting equations. The stability of the equilibria may be determined from analysing the eigenvalues of the Jacobian $\boldsymbol{J}$ (given in Appendix A) when evaluated at equilibrium. Any equilibrium will be asymptotically (locally) stable only if the real parts of all eigenvalues of $\boldsymbol{J}$ are negative.

3. Equilibrium and stability analysis

The above model has an "infection-free" equilibrium in which $I_c^* = I_a^* = 0$. Substituting these values into Eq. (3) one finds that the population consists entirely of susceptible individuals:

$$S_c^* = N_c^* = \frac{\mu}{\alpha + \mu}, \quad S_a^* = N_a^* = \frac{\alpha}{\alpha + \mu}.$$

As newborns are not exposed to infections there are no recovered individuals and $R_c^* = R_a^* = 0$. Inserting these values into the Jacobian of Appendix A, yields the matrix $\boldsymbol{J}$ having five eigenvalues, three of which are negative: $\lambda_{1,2} = -\alpha - \mu$, $\lambda_3 = -\mu$. The remaining two eigenvalues are solutions of the determinental equation:

$$\begin{vmatrix} \beta_{cc} - \gamma_c - \mu - \lambda & \beta_{ca} \\ \beta_{ac} & \beta_{aa} - \gamma_a - \mu - \lambda \end{vmatrix} = 0.$$

This is a simple quadratic in λ, and the necessary and sufficient condition for the eigenvalues to have negative real parts is that the following two inequalities are satisfied:

$$\beta_{cc} + \beta_{aa} - 2\mu - \gamma_c - \gamma_a < 0, \tag{4a}$$

$$(\beta_{cc} - \gamma_c - \mu)(\beta_{aa} - \gamma_a - \mu) - \beta_{ca}\beta_{ac} > 0. \tag{4b}$$

The two latter conditions ((4a) and (4b)) are thus the necessary and sufficient conditions for local stability of the infection free equilibrium state.

As an example, Fig. 5 plots the $\beta_{cc} - \beta_{aa}$ parameter space at which the infection free equilibrium is stable under the constraint that $\beta_{ca} = \beta_{ac} = 10$. As Fig. 5 shows, for this particular case, the first constraint (4a) is redundant while the second (4b), the shaded region fully defines the locally stable regime.

An equivalent approach for determining the stability of the infection-free equilibrium may be obtained by calculating the so-called "next generation matrix" A. Beginning with a vector v of infecteds in the two classes (children/adults), one can find the number of newly infected individuals in the next generation in the two classes via:

$$v' = \begin{bmatrix} R_{0cc} & R_{0ca} \\ R_{0ac} & R_{0aa} \end{bmatrix} v = Av.$$

As shown in Appendix B, the next generation matrix A has entries:

$$R_{0cc} = \beta_{cc}/(\gamma_c + \mu), \quad R_{0aa} = \beta_{aa}/(\gamma_a + \mu),$$
$$R_{0ca} = \beta_{ca}/(\gamma_a + \mu), \quad R_{0ac} = \beta_{ac}/(\gamma_c + \mu).$$

These expressions are based on the total amount of infections caused by each class over the lifetime of the infection. For example, R_{0ca} represents the average number of secondary infections in the subpopulation of children produced by an adult infective per unit time. The reproductive number R_0 is the dominant eigenvalue of the next generation matrix A, and the infection free equilibrium is stable if

$$R_0 < 1. \tag{5a}$$

Such a condition implies that on average each infection gives rise to less than one new infection in the next generation and therefore the disease must eventually die out.

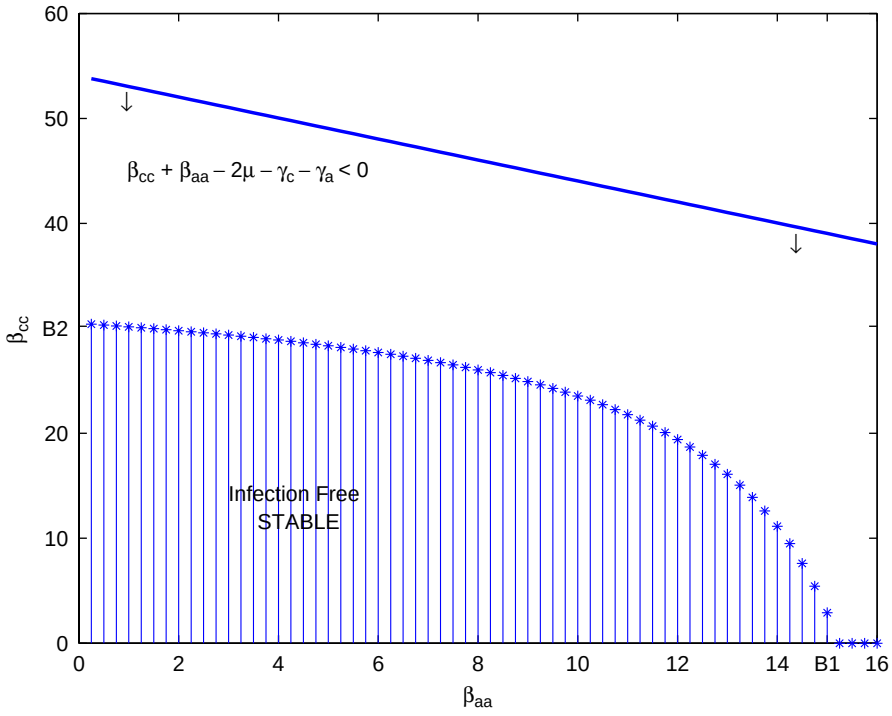

Fig. 5. Schematical view of stability boundaries for infection free equilibrium. The adult contact rate β_{aa} is given on the horizontal axis while the child contact rate β_{cc} is given on the vertical axis. The points B1 = 15.24 (for β_{aa}) and B2 = 30.47 (for β_{cc}) are critical contact rates calculated from Eq. (4b). The model parameters used are $\beta_{ac} = \beta_{ca} = 10$, $\mu = 0.02$, $\alpha = 0.5$, $\gamma_c = 36$ and $\gamma_a = 18$.

The dominant eigenvalue of A can be found from the characteristic equation

$$R_0^2 - (R_{0cc} + R_{0aa})R_0 + R_{0cc}R_{0aa} - R_{0ca}R_{0ac} = 0$$

and so

$$R_0 = \frac{1}{2}\left\{(R_{0cc} + R_{0aa}) + \sqrt{(R_{0cc} - R_{0aa})^2 + 4R_{0ca}R_{0ac}}\right\}. \tag{5b}$$

It can be shown that $R_0 < 1$ is equivalent to the result found from the eigenvalues analysis (conditions (4a) and (4b)) above. For example, the condition reproduces the borders of the stability curve in Fig. 5. Note that if $R_{0ac} = R_{0ca} = 0$, one sees easily from condition (5) that the system will be stable if both $R_{0cc} < 1$ and $R_{0aa} < 1$, a feature we will see again below.

4. A simplified model

It is difficult to gain any further analytical insights into the dynamics of Eq. (3) directly. However, it is possible to examine the case $\beta_{ca} = \beta_{ac} = 0$ where there is no significant contact between child and adult age classes. This is a reasonable first approximation that allows us to make important analytical insights regarding the mechanism underlying the model's dynamics. Eq. (3) becomes:

$$\begin{aligned}
\frac{dS_c}{dt} &= \mu - \left(\alpha + \mu + \frac{\beta_{cc}}{N_c} I_c\right) S_c, \\
\frac{dS_a}{dt} &= \alpha S_c - \left(\mu + \frac{\beta_{aa}}{N_a} I_a\right) S_a, \\
\frac{dI_c}{dt} &= \frac{\beta_{cc}}{N_c} I_c S_c - (\gamma_c + \mu) I_c, \\
\frac{dI_a}{dt} &= \frac{\beta_{aa}}{N_a} I_a S_a - (\gamma_A + \mu) I_a, \\
\frac{dR_c}{dt} &= \gamma_c I_c - (\alpha + \mu) R_c,
\end{aligned} \tag{6}$$

with

$$N_c + N_a = 1.$$

The ODE system (6) has four equilibria which may be found by setting all rates in Eq. (6) to zero. There are four possible equilibrium solutions E_1, E_2, E_3 and E_4 and these are given in full in Table 1. As can be found by summing separately over each age class in Eq. (6), all equilibria have the property that:

$$N_c^* = \frac{\mu}{\alpha + \mu}, \quad N_a^* = \frac{\alpha}{\alpha + \mu},$$

where N_c^* and N_a^* represent the equilibrium value of N_c and N_a, respectively.

Table 1
The four equilibrium solution for the system (3)

	S_c^*	S_a^*	I_c^*	I_a^*	c^*	a^*
E_1	$N_c^* = \frac{\mu}{\alpha+\mu}$	$N_a^* = \frac{\alpha}{\alpha+\mu}$	0	0	0	0
E_2	$\frac{(\mu+\gamma_c)N_c^*}{\beta_{cc}}$	$\frac{(\mu+\gamma_c)N_a^*}{\beta_{cc}}$	$\frac{\mu}{(\mu+\gamma_c)} - \frac{\mu}{\beta_{cc}}$	0	$\frac{\gamma_c I_c^*}{\alpha+\mu}$	$\frac{\gamma_c N_a^*}{\alpha+\mu}$
E_3	$\frac{\mu}{\alpha+\mu}$	$\frac{(\mu+\gamma_a)N_a^*}{\beta_{aa}}$	0	$\left[\frac{1}{(\mu+\gamma_a)} - \frac{1}{\beta_{aa}}\right]\mu N_a^*$	0	$\frac{\gamma_a I_a^*}{\mu}$
E_4	$\frac{(\mu+\gamma_c)N_c^*}{\beta_{cc}}$	$\frac{(\mu+\gamma_a)N_a^*}{\beta_{aa}}$	$\frac{\mu}{(\mu+\gamma_c)} - \frac{\mu}{\beta_{cc}}$	$\left[\frac{(\mu+\gamma_c)}{\beta_{cc}(\mu+\gamma_a)} - \frac{1}{\beta_{aa}}\right]\mu N_a^*$	$\frac{\gamma_c I_c^*}{\alpha+\mu}$	$\frac{\alpha R_c^* + \gamma_a I_a^*}{\mu}$

The stability properties of the equilibria are now examined in turn.

E_1: The "infection-free" equilibrium in which $I_c^* = I_a^* = 0$ (see Table 1). From the Jacobian (Appendix A) one finds that the equilibrium is asymptotically stable only if the basic reproduction numbers satisfy:

$$R_{0cc} = \frac{\beta_{cc}}{\mu+\gamma_c} < 1 \quad \text{and} \quad R_{0aa} = \frac{\beta_{aa}}{\mu+\gamma_a} < 1. \tag{7}$$

Note that this is identical to Eq. (4b) for the parameters used here.

E_2: The equilibrium in which $I_a^* = 0$; all other subpopulations have positive equilibrium values (see Table 1). The equilibrium is found to be locally stable if:

$$R_{0cc} = \frac{\beta_{cc}}{\mu+\gamma_c} > 1 \quad \text{and} \quad R_{0aa} = \frac{\beta_{aa}(\mu+\gamma_c)}{\beta_{cc}(\mu+\gamma_a)} < 1. \tag{8}$$

Note that the condition $R_{0cc} > 1$ corresponds exactly to the condition that $I_c^* > 0$, as can be seen by referring to Table 1.

E_3: The equilibrium with $I_c^* = 0$; all other subpopulations have positive equilibrium (see Table 1). The equilibrium is locally stable if:

$$R_{0cc} = \frac{\beta_{cc}}{\mu+\gamma_c} < 1 \quad \text{and} \quad R_{0aa} = \frac{\beta_{aa}}{\mu+\gamma_a} > 1. \tag{9}$$

Here the condition $R_{0aa} > 1$ corresponds to $I_a^* > 0$ (see Table 1).

E_4: The "epidemic equilibrium" where both children and adult equilibrium populations are positive $I_c^* > 0$ and $I_a^* > 0$. The conditions for a locally stable equilibrium are:

$$R_{0cc} = \frac{\beta_{cc}}{\mu+\gamma_c} > 1 \quad \text{and} \quad R_{0aa} = \frac{\beta_{aa}(\mu+\gamma_c)}{\beta_{cc}(\mu+\gamma_a)} > 1. \tag{10}$$

Conditions (7)–(10) can be summarized in terms of the critical values for the contact rate:

$$\beta_{cc}^\dagger = \mu + \gamma_c \quad \text{for all equilibria},$$

$$\beta_{aa}^\dagger = \begin{cases} \mu+\gamma_a & \text{for } E_1 \text{ and } E_3, \\ \dfrac{\mu+\gamma_a}{\mu+\gamma_c}\beta_{cc} & \text{for } E_2 \text{ and } E_4. \end{cases}$$

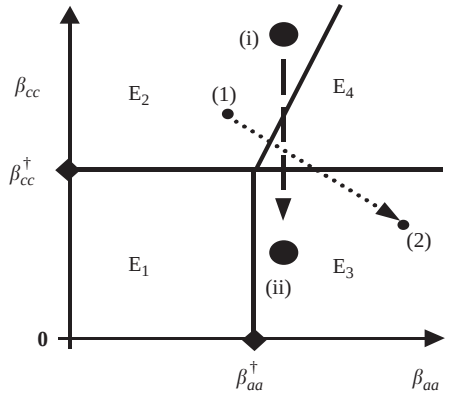

Fig. 6. Schematical view of boundaries of stability for each of the four equilibria E_1, E_2, E_3, E_4 with $\beta_{ac} = \beta_{ca} = 0$. The adult contact rate β_{aa} is given on the horizontal axis while the child contact rate β_{cc} is given on the vertical axis. The critical contact rates $(\beta_{aa}^\dagger, \beta_{cc}^\dagger)$, divide the parameter space into four regions in which each of the equilibrium points are locally stable. The diagonal line dividing regions E_2 and E_4 derives from condition (11). As discussed in the text, a change in contact rate may cause a switch between equilibria and lead to epidemic outbreak. The dotted and dashed lines illustrate how changes in contact rate result in a transition from equilibrium E_2 to E_3 (points 1–>2, or I–>ii).

Note that for the model parameters used here: $\beta_{cc}^\dagger = 36.02$ (for all equilibria) and $\beta_{aa}^\dagger = 18.02$ (for E_1 and E_3). These critical values divide the $\beta_{cc} - \beta_{aa}$ parameter space into four different regions that specify where each equilibrium is stable.

$$\begin{aligned} E_1&: \ \beta_{cc} < \beta_{cc}^\dagger \quad \beta_{aa} < \beta_{aa}^\dagger, \\ E_2&: \ \beta_{cc} > \beta_{cc}^\dagger \quad \beta_{aa} < \frac{\mu+\gamma_a}{\mu+\gamma_c}\beta_{cc}, \\ E_3&: \ \beta_{cc} < \beta_{cc}^\dagger \quad \beta_{aa} > \beta_{aa}^\dagger, \\ E_4&: \ \beta_{cc} > \beta_{cc}^\dagger \quad \beta_{aa} > \frac{\mu+\gamma_a}{\mu+\gamma_c}\beta_{cc}. \end{aligned} \tag{11}$$

The four regions of stability are shown schematically in Fig. 6. This should be compared to Fig. 5 calculated for the special case $\beta_{ca} = \beta_{ac} = 10$. Note how the regime of the infection free equilibrium remains qualitatively similar indicating the model analysis has a good degree

of robustness even though it is based on the restriction $\beta_{ca} = \beta_{ac} = 0$.

5. Threshold effects in the simplified model

The above model offers an explanation for the unusual transition seen in Fig. 1 with regard to paralytic cases of polio, and more generally with regard to "diseases of development". Fig. 1 shows that before the 20th century relatively few cases of polio were observed, while after 1906 there is a sustained epidemic of the disease. This may be understood in light of the model's different equilibria. It is believed that the pre-epidemic period was characterized by a relatively high contact rate among children. In particular, children under 2 years of age create a microenvironment of less than optimal hygiene within the family and within daycare settings, readily facilitating fecal–oral and oral–oral (mouth–fingers–mouth) transmission (WHO, 1993). The spreading of the poliovirus between families was also intensive with multiple families often sharing the same toilets or privies (Melnick and Ledinko, 1953). As the disease spread among children in this period, we assume that $R_{0cc} > 1$ (or equivalently $\beta_{cc} > \beta_{cc}^{\dagger}$). On the other hand, since the adult population had a minor impact on the disease transmission, with very few paralytic cases it can be assumed that $R_{0aa} < 1$ (or equivalently $\beta_{aa} < \beta_{aa}^{\dagger}$). The above parameter range corresponds to stable equilibrium E_2 with $I_c^* > 0$ and $I_a^* = 0$, while all other equilibria are unstable.

Fig. 7 shows a typical simulation in this parameter range where the children's contact rate $\beta_{cc} = 90$ is larger than the critical threshold level ($\beta_{cc}^{\dagger} = 32.02$), while $\beta_{aa} = 40$ is less than critical level for E_2 in Eq. (8) ($\beta_{aa}^{\dagger} = 40.0278$). Similar results are obtained for smaller values of β_{aa}, as long as they are less than the critical value. The infection in the adult population reaches extinction while the number of infected children attains a positive endemic level. Both from Table 1 and the numerical simulation, it is evident that model populations converge to the stable equilibrium:

$$E_2 : S_c^* = 0.0355, \quad S_a^* = 0.3550,$$
$$I_c^* = 0.0003, \quad I_a^* = 0,$$
$$R_c^* = 0.0554, \quad R_a^* = 0.5538.$$

Immune adults in the recovered group R_a^* are much greater in number than in all other groups. This is because nearly all children become immune after infection, and pass to the recovered group (first to R_c and later to R_a) where they enjoy long life immunity to poliovirus. Although the number of susceptible adults is appreciable, it is less than that required to generate an epidemic in the adult population.

As already discussed, in the late 19th and at the beginning of the 20th century various noteworthy improvements in hygiene took place. The most prominent development was the separation of central sewage from drinking water. These improvements led to the creation of a cleaner environment greatly reducing the probability of becoming infected at an early age.

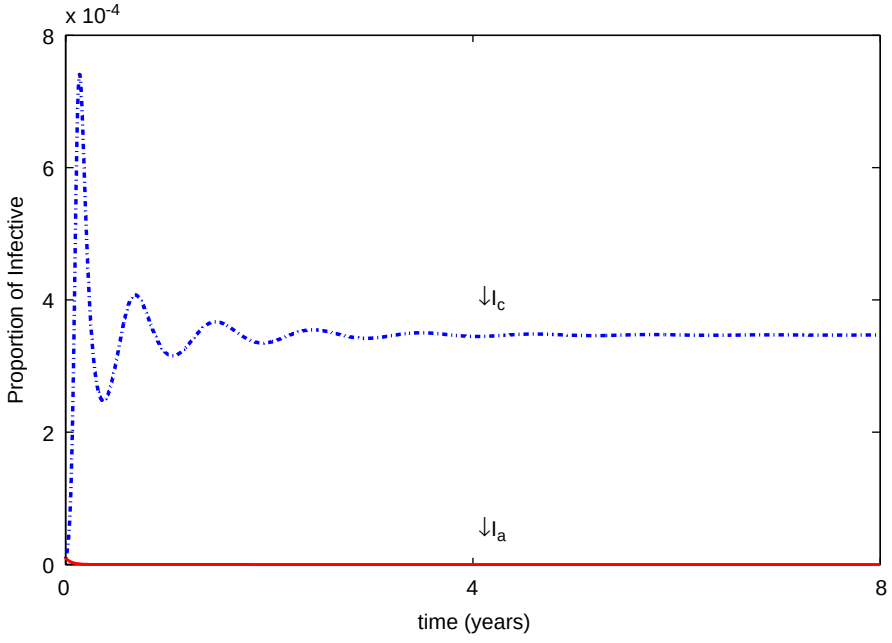

Fig. 7. Time-series of infectious population when $I_c^* > 0$ and $I_a^* = 0$ (E_2) with $\beta_{cc} = 90$, $\beta_{aa} = 40$, $\beta_{ac} = \beta_{ca} = 0$). The simulation uses the standard model parameters with $\mu = 0.02$, $\alpha = 0.5$, $\gamma_c = 36$ and $\gamma_a = 18$.

In Fig. 6, we designate an analogous transition in terms of the model parameters at point (i) with $\beta_{cc} > \beta_{cc}^{\dagger}$ to parameters at point (ii) with $\beta_{cc} < \beta_{cc}^{\dagger}$. The transition reflects a significant reduction in the children's contact rate for a given adult contact rate $\beta_{aa} > \beta_{aa}^{\dagger}$. As Fig. 6 shows, moving from point (i) to (ii) corresponds to passing from equilibrium E_2 to E_3. With the reduction in the disease transmission rate β_{cc}, the number of susceptible children is able to grow eventually building up a larger pool of susceptible adults.

Fig. 8 shows the model's dynamics when the children's contact rate is decreased from $\beta_{cc} = 160$ to $\beta_{cc} = 16$, and the system moves from E_2 to E_3. When the susceptible adults reach a critical level, an outbreak occurs and the number of infected adults increases dramatically. Note that during the epidemic, the infectives can reach to some 4–5% of the population and a large number of paralytic cases can be expected. These results are in line with the situation observed in Fig. 1 after 1906 where major outbreaks in the United States were caused by a gradual increase of susceptible adults reaching a critical mass by 1906 (Sutter et al., 1999). Returning to the model simulation in Fig. 8, one sees that after the epidemic the populations reach the stable equilibrium:

$$E_3 : S_c^* = 0.0294, \quad S_a^* = 0.4373, \quad I_c^* = 0,$$
$$I_a^* = 0.0006, \quad R_c^* = 0, \quad R_a^* = 0.5327.$$

At this equilibrium there are no infected or recovered children. Thus no children have immunity and move on to leave a large susceptible adult population whose individuals have never been exposed to polio.

To demonstrate that this behavior is not an artifact of the assumption that contact rates between child and adult groups are negligible, the simulation was repeated for the full model with $\beta_{ca} = \beta_{ac} = 10$. The model's dynamics are displayed in Fig. 9 and there are no qualitative differences from that seen in Fig. 8. In short the results appear to be reasonably robust to the simplifications used as was confirmed from a wide range of similar comparative tests.

6. Indirect poliovirus transmission via environmental factors

The SIR model is based on the conventional direct transmission route of diseases in well mixed populations where infections are passed on through random contact between susceptible and infected individuals. This is controlled by the contact rates (β_{ij}) in Eq. (6), which in the main, covers direct disease transmission through the oral–oral and fecal–oral routes. However, poliomyelitis is also transmitted indirectly through a common vehicle or via the surrounding environment without direct contact (e.g. via sewage, food, water).

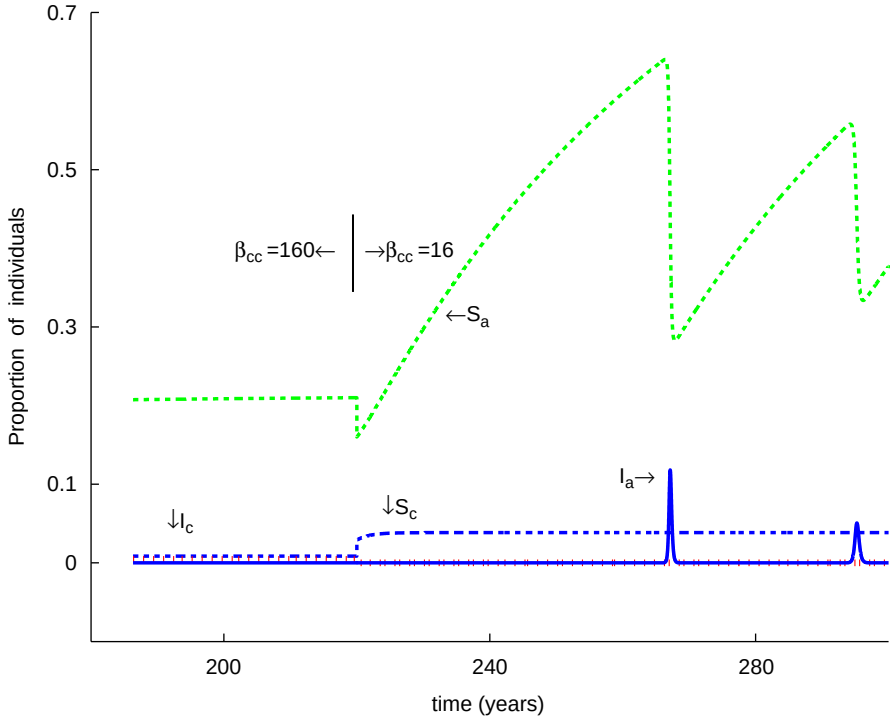

Fig. 8. Time series of susceptible (dashed line) and infectious (solid and dotted lines) population. The simulation begins with all subpopulations at values given by E_2 ($I_c^* > 0$ and $I_a^* = 0$, $\beta_{cc} = 160$, $\beta_{aa} = 40$, $\beta_{ac} = \beta_{ca} = 0$). At $t = 220$ the contact rate $\beta_{cc} = 160$ was intentionally reduced to $\beta_{cc} = 16$ where the population trajectories are attracted to E_3 ($I_c^* = 0$ and $I_a^* > 0$). In the process a polio outbreak is triggered at $t = 270$ (to aid visualization we have scaled infectives by a factor of three). Parameters as in Fig. 7.

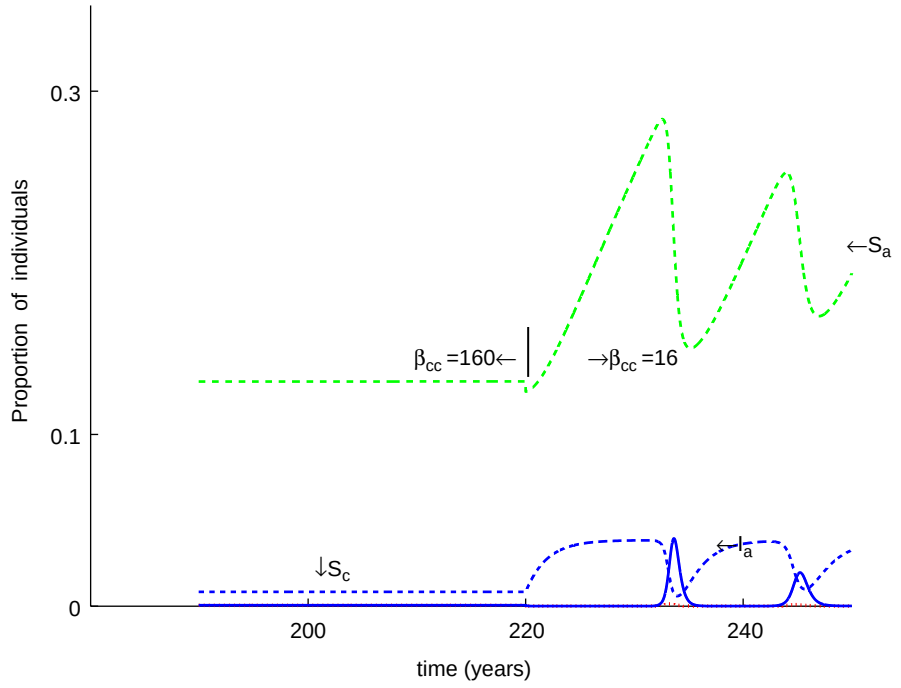

Fig. 9. Time series of susceptible (dashed lines) and infectious (solid and dotted lines) population. The simulation begins with all subpopulations at equilibrium ($I_c^* = 0.125$ and $I_a^* = 0$, $\beta_{cc} = 160$, $\beta_{aa} = 40$, $\beta_{ac} = \beta_{ca} = 0$). At $t = 220$ the contact rate $\beta_{cc} = 160$ was intentionally reduced to $\beta_{cc} = 16$ where the population triggered to polio outbreak is at $t = 235$ (To aid visualization we have scaled infectives by a factor of three). Other parameters as in Fig. 7.

The parameter ε may be used to investigate the influence of such an "environmental factor". As seen in Fig. 4 the environmental factor is modeled by allowing susceptible individuals to pass directly to the infected stage at the rate εS, without requiring contact with infective individuals. After incorporating ε to Eq. (6), the model becomes:

$$\begin{aligned}
\frac{dS_c}{dt} &= \mu - \left(\varepsilon + \alpha + \mu + \frac{\beta_{cc}}{N_c} I_c\right) S_c,\\
\frac{dS_a}{dt} &= \alpha S_c - \left(\varepsilon + \mu + \frac{\beta_{aa}}{N_a} I_a\right) S_a,\\
\frac{dI_c}{dt} &= \left(\varepsilon + \frac{\beta_{cc}}{N_c} I_c\right) S_c - (\gamma_c + \alpha + \mu) I_c,\\
\frac{dI_a}{dt} &= \left(\varepsilon + \frac{\beta_{aa}}{N_a} I_a\right) S_a - (\gamma_a + \mu) I_a + \alpha I_c,\\
\frac{dR_c}{dt} &= \gamma_c I_c - (\alpha + \mu) R_c. \qquad (12)
\end{aligned}$$

The parameter ε allows provision for a clean environment with $\varepsilon = 0$, or a hostile environment with $\varepsilon > 0$ in which there might be low hygiene, poor living conditions and large families. It is assumed that ε is large in undeveloped societies and tends to decrease with development.

Fig. 10 graphs the infected equilibrium numbers I_c^* and I_a^* as a function of ε. The figure makes clear that the equilibrium number of infected adults increases as the environment becomes cleaner (i.e. ε reduces), as predicted for diseases of development. When infection through the environmental routes increase (i.e. ε increases) the equilibrium number of infected children increases, thereby providing greater immunity to these individuals as adults, again as expected for diseases of development.

The influence of ε on the equilibrium populations can also be predicted qualitatively with a simple perturbation technique. Firstly, define the equilibrium solution of Eq. (12) when $\varepsilon = 0$ as $(S_{c0}^*, S_{a0}^*, I_{c0}^*, I_{a0}^*)$. Now for small $\varepsilon > 0$, the equilibrium solution is

$$\begin{aligned}
&S_c^*(\varepsilon) = S_{c0}^* + \Delta s_c(\varepsilon) \;\; S_a^*(\varepsilon) = S_{a0}^* + \Delta s_a(\varepsilon)\\
&I_c^*(\varepsilon) = I_{c0}^* + \Delta i_c(\varepsilon) \;\; I_a^*(\varepsilon) = I_{a0}^* + \Delta i_a(\varepsilon), \qquad (13)
\end{aligned}$$

where Δs_c, Δs_a, Δi_c, Δi_a are relatively small perturbations.

After inserting Eq. (13) into ODE system (12), and eliminating second-order effects one finds:

$$\begin{aligned}
&\Delta s_c \propto \varepsilon,\\
&\Delta i_c \propto \varepsilon,\\
&\Delta i_a \propto -\varepsilon.
\end{aligned}$$

Therefore, if ε increases then (a) Δi_C, the number of infected children, must also increase; and (b) Δi_a, the number of infected adults, must decrease, confirming the trends seen in Fig. 10.

Another effect of the environmental parameter may be seen in Fig. 11 where the model has been simulated with three different values of ε. When ε is small

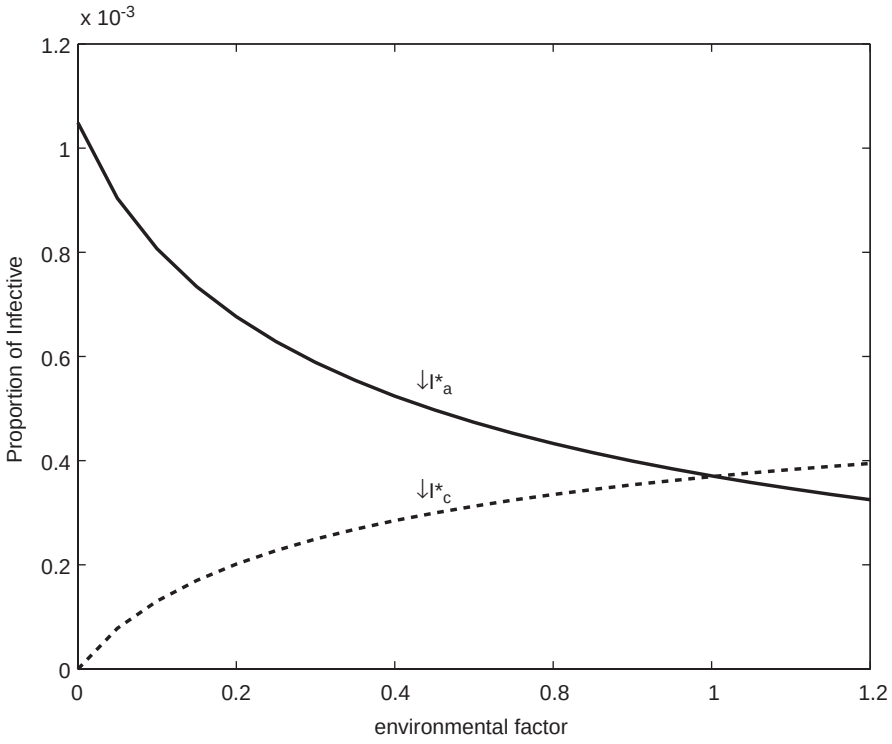

Fig. 10. Equilibrium numbers of infective individuals I_c^* (dashed line) and I_a^* (solid line) as a function of the environmental factor ε. Parameters for simulation use are as in Fig. 7.

($\varepsilon = 0.0002$, i.e. in a very clean environment), there is a strong outbreak in the adult population I_a. As ε increases ($\varepsilon = 0.3$) the outbreaks become severely damped or even non-existent. This is once again a feature of "diseases of development", i.e. only at higher level of industrial and social development (when ε decreases) can large outbreaks take place.

The latter phenomenon can be explained in terms of the eigenvalues of the Jacobian of system (12) about equilibrium. For the large parameter ranges examined here, at most two eigenvalues were found to have imaginary components. The positive imaginary component is plotted as a function of ε in Fig. 12. The existence of the imaginary components in the eigenvalues is of great significance because it causes oscillations (i.e. epidemics) in the time dependent graph of infectives (see Fig. 11). Fig. 12 shows that there is another interesting threshold effect. When ε is larger than the critical value $\varepsilon_c = 0.008$, all eigenvalues lack an imaginary component and thus epidemics are inhibited. This has the very interesting and counterintuitive interpretation that in developing countries the substantial indirect transmission routes can actually serve to prevent outbreaks.

7. Discussion

The above model offers an explanation for the extraordinary jump in the number of paralytic polio cases that emerged at the beginning of the 20th century and the epidemics that followed with development. As Fig. 1 shows, the increase in cases appears to be similar to a threshold effect, a feature which is intrinsic to the epidemic model outlined here. The threshold is shown to be a specific outcome of an interplay between the dynamics of the two age classes within the population and governed by the contact rates within each class. With development, improvements in sanitation reduced the transmissibility of the disease. As such, children were no longer exposed to the polio virus at an early age, and thus remained susceptible to the disease as older children or even adults. This led to the transformation of polio from endemic to epidemic in the early 20th century. The mechanism has some similarity to the "honeymoon period" that is observed after mass vaccinations in which a decrease of cases is observed whilst a reservoir of susceptibles builds up slowly in the population (Scherer and McLean, 2002). When susceptibles eventually reach a critical level, an epidemic outbreak is triggered. The analogy with polio is through sanitation which acts to create a slow build up of unexposed children and thus susceptible adults.

Previous theoretical discussions of polio usually framed the disease dynamics in terms of the average age of infection in the population (Hillis, 1979; Anderson and May, 1991). As the average age of infection rises, those who acquire the infection are older and, having a larger case:incidence ratio, are more prone

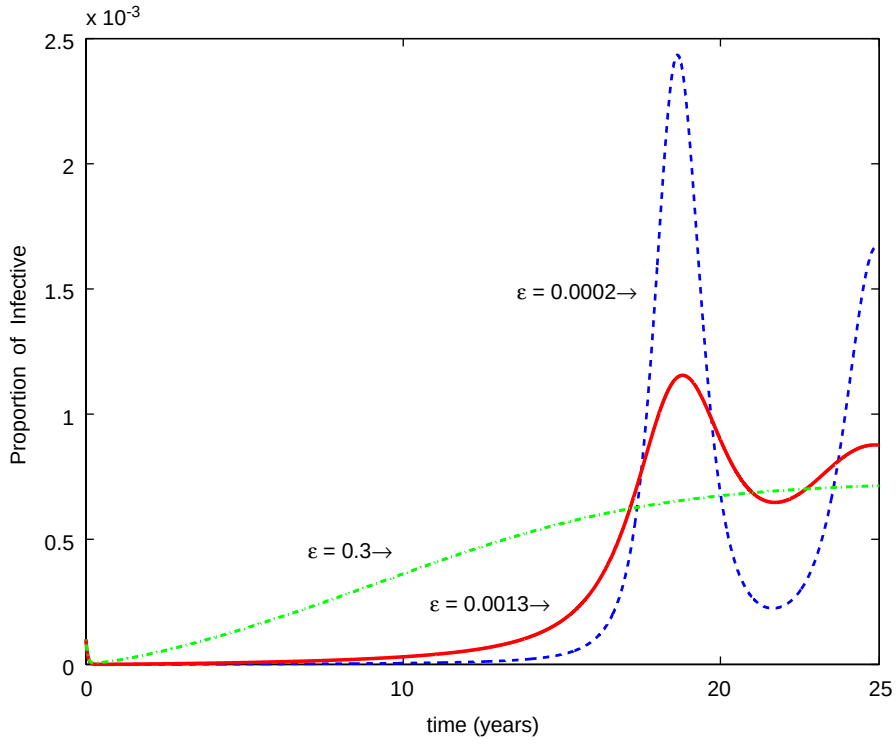

Fig. 11. Time series of infectious adults (I_a) with $\varepsilon = 0.0002$ (dotted line), $\varepsilon = 0.0013$ (solid line) and $\varepsilon = 0.3$ (dashed line). The simulation uses the standard model parameters with contact rates $\beta_{cc} = 32$, $\beta_{aa} = 73$.

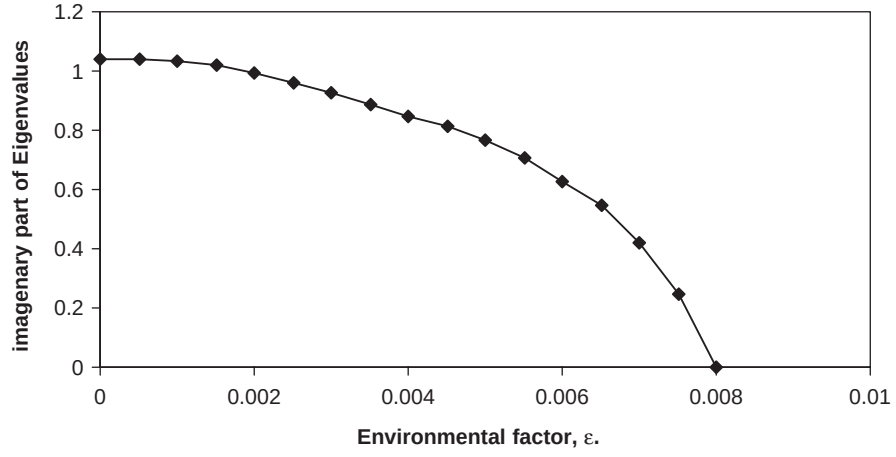

Fig. 12. Graph of eigenvalues's imaginary part Im(λ) as function of environmental factor ε.

to paralysis and serious medical complications. However, this view does not in itself explain the non-equilibrium epidemic dynamics nor the threshold phenomenon. The two age-class model described here is able to reproduce epidemic dynamics without even needing to take into account that the case:incidence ratio increases with age—something that is in any case controversial (Nathanson and Martin, 1979; Sabin, 1981). Finally, the model gives an explanation based solely on the contact rate parameters of the various subpopulations. This seems to be preferable to compound variables such as the age at first infection which is a complex composite index that summarises the state of severable variables.

More recent attempts at understanding poliomyelitis have led to the development of the exposure intensity polio model (Nielsen et al., 2001). According to this theory, the severity of infectious polio disease depends on intensity of exposure. Thus when an infectee brings polio into the home, close and constant contact with

other family members, especially younger brothers and sisters, can lead to severe and often paralytic cases. Nielsen et al. (2001) argue that this helps explain the puzzling rise in the number of younger children found paralyzed in the 1950s. Future directions in modeling diseases such as polio might benefit by combining the exposure intensity polio model with spatially structured population networks (e.g. the household models of Becker and Dietz (1995), or small world models of Watts and Strogatz (1998)). The effects of social structures (Keeling et al., 1997) and localized population aggregations will no doubt have significant impact on disease transmission.

Of course, in this particular fascinating story of the poliovirus, we cannot forget that with development also came vaccinations. With the widespread introduction of inactivated polio vaccines (IPV) in 1955, the phenomenon of massive paralytical outbreaks appeared to come to an end. In 1961, an oral polio vaccine (OPV) became available. It soon became the vaccine of choice for the control of polio and led to the idea that the disease of poliomyelitis could be totally eradicated. In 1988, the World Health Organization (WHO) resolved to embark on a campaign to eradicate polio from the world by 2000 (World Health Assembly, 1988). Although the goal was not achieved by 2000, polio cases have dropped by 95% around the world and a new deadline has been set to eradicate polio by 2005 (WHO, 2003). Nevertheless there is speculation that this deadline may be somewhat optimistic (Heymann et al., 2005) and complete eradication of polio might not yet be within grasp, or might even be impossible. While these eradication deadlines are being set, new and severe epidemic outbreaks of polio are taking place in Nigeria raising the possibility of a continent-wide disaster in Africa (Roberts, 2004).

Acknowledgements

We thank Professors Manfred Green, Danny Cohen and Tiberio Swartz for helpful comments and suggestions. We are grateful to Ronen Olinky, Eliezer Shochat, David Bunimovich and Shimon Zeldner for fruitful and stimulating discussions. In addition, we gratefully acknowledge and helpful suggestions of Vincent Jansen and three anonymous reviewers, one of whom suggested the "next generation matrix" approach. The work was supported by the James S McDonnell Foundation.

Appendix A

The Jacobian $\boldsymbol{J}$ is obtained by linearizing Eq. (3) about equilibrium, and is used for studying the local stability of the system. A calculation shows that

$$J=\begin{pmatrix} a_{11} & 0 & a_{13} & a_{14} & a_{15} \\ \alpha & a_{22} & a_{23} & a_{24} & 0 \\ a_{31} & 0 & a_{33} & a_{34} & a_{35} \\ 0 & a_{42} & a_{43} & a_{44} & 0 \\ 0 & 0 & \gamma_c & 0 & -\alpha-\mu \end{pmatrix}$$

$$a_{11}=-\alpha-\mu-a_{31},$$

$$a_{31}=-\frac{\beta_{cc}I_c^*S_c^*}{(N_c^*)^2}+\frac{\beta_{cc}I_c^*}{N_c^*}-\frac{\beta_{ca}I_a^*S_c^*}{(N_c^*)^2}+\frac{\beta_{ca}I_a^*}{N_c^*},$$

$$a_{22}=-\mu-a_{42},$$

$$a_{42}=-\frac{\beta_{aa}I_a^*S_a^*}{(N_a^*)^2}+\frac{\beta_{aa}I_a^*}{N_a^*}-\frac{\beta_{ac}I_c^*S_a^*}{(N_a^*)^2}+\frac{\beta_{ac}I_c^*}{N_a^*},$$

$$a_{13}=\frac{\beta_{cc}I_c^*S_c^*}{(N_c^*)^2}-\frac{\beta_{cc}S_c^*}{N_c^*},\quad a_{23}=\frac{\beta_{ac}I_c^*S_a^*}{(N_a^*)^2}-\frac{\beta_{ac}S_a^*}{N_a^*},$$

$$a_{33}=-\gamma_c-\mu-a_{13},\quad a_{34}=-a_{23},$$

$$a_{14}=-\frac{\beta_{ca}S_c^*}{N_c^*}+\frac{\beta_{ca}I_a^*S_c^*}{(N_c^*)^2},\quad a_{24}=\frac{\beta_{aa}I_a^*S_a^*}{(N_a^*)^2}-\frac{\beta_{aa}S_a^*}{N_a^*},$$

$$a_{34}=-a_{14},\quad a_{44}=-\gamma_a-\mu-a_{24},$$

$$a_{15}=\frac{\beta_{cc}I_c^*S_c^*}{(N_c^*)^2}+\frac{\beta_{ca}I_a^*S_c^*}{(N_c^*)^2},\quad a_{35}=-a_{15}.$$

Appendix B

The next generation matrix is found following the recipe given in Van den Driessche and Watmough (2002). Let F_i be the rate of appearance of new infections in compartment i, V_i^+ be the rate of transfer of individuals by all other means, and V_i^- be the rate of transfer of individuals out of compartment i. One can write Eqs. (3) in the form

$$\frac{\mathrm{d}x_i}{\mathrm{d}t}=f_i(x)=F_i(x)-V_i(x),$$

where $V_i=V_i^--V_i^+$. In the case of Eqs. (3), the vector $\underline{F}=(F_i)$ and $\underline{V}=(V_i)$ can be written as

$$\underline{F}=[0,0,(\beta_{cc}/N_cI_c+\beta_{ca}/N_cI_a)S_c,\\ (\beta_{ac}/N_aI_c+\beta_{aa}/N_aI_a)S_a,0],$$

$$\underline{V}=[\alpha+\mu+\beta_{cc}/N_cI_c+\beta_{ca}/N_cI_a)S_c,\\ -\alpha S_c+(\mu+\beta_{aa}/N_aI_a+\beta_{ac}/N_aI_c)S_a,\\ (\gamma_c+\mu)I_c,(\gamma_a+\mu)I_a,-\gamma_cI_c+(\alpha+\mu)R_c].$$

For the infection free equilibrium, we focus on the variables I_c and I_a since they are both zero at equilibrium. Now form the matrix of partial derivatives

(evaluated at equilibrium) with respect to I_c and I_a in the third and fourth components of the vector $\underline{F}$ (and $\underline{V}$) giving the matrix $\underline{\underline{P}}$ (and $\underline{\underline{Q}}$).

$$\underline{\underline{P}} = \begin{bmatrix} \beta_{cc} & \beta_{ca} \\ \beta_{ac} & \beta_{aa} \end{bmatrix}, \quad \underline{\underline{Q}} = \begin{bmatrix} \gamma_c + \mu & 0 \\ 0 & \gamma_a + \mu \end{bmatrix}.$$

The next generation matrix is defined as (Van den Driessche and Watmough, 2002):

$$\underline{\underline{P}}\,\underline{\underline{Q}}^{-1} = \begin{bmatrix} \beta_{cc} & \beta_{ca} \\ \beta_{ac} & \beta_{aa} \end{bmatrix} \begin{bmatrix} 1/(\gamma_c + \mu) & 0 \\ 0 & 1/(\gamma_a + \mu) \end{bmatrix} = \begin{bmatrix} \beta_{cc}/(\gamma_c + \mu) & \beta_{ca}/(\gamma_a + \mu) \\ \beta_{ac}/(\gamma_c + \mu) & \beta_{aa}/(\gamma_a + \mu) \end{bmatrix} = \begin{bmatrix} R_{0cc} & R_{0ca} \\ R_{0ac} & R_{0aa} \end{bmatrix}.$$

References

Anderson, R.M., May, R.M., 1991. Infectious Diseases of Humans: Dynamics and Control. Oxford University Press, Oxford, pp. 114–116.

Becker, N.G., Dietz, K., 1995. The effect of household distribution on transmission and control of highly infectious-diseases. Math. Biosci. 127 (2), 207–219.

Coleman, P.G., Perry, B.D., Woolhouse, M.E.J., 2001. Endemic stability—a veterinary idea applied to human public health. Lancet 357, 1284–1286.

Cvjetanovic, B., Grab, B., Dixon, H., 1982. Epidemiological models of poliomyelitis and measles and their application in the planning of immunization programmes. Bull. W.H.O. 60, 405–422.

Dowdle, W.R., Birmingham, M.E., 1997. The biologic principles of poliovirus eradication. J. Infect. Dis. 175, S286–S292.

Heymann, D.L., Sutter, R.W., Aylward, R.B., 2005. A global call for new polio vaccines. Nature 434, 699–700.

Hillis, A., 1979. A mathematical model for the epidemiologic study of infectious diseases. Int. J. Epidemiol. 8, 167–176.

Jacquez, J., Simon, C., Koopman, J., 1995. Core groups and the R_0s for subgroups in heterogeneous SIS and SI models. In: Mollison, D. (Ed.), Epidemic Models: Their Structure and Relation to Data. Cambridge University Press, Cambridge, UK, pp. 279–301.

Keeling, M.J., Rand, D.A., Morris, A.J., 1997. Correlation models for childhood epidemics. Proc. R. Soc. London B 266 (1385), 1149–1156.

Krause, R.M., 1998. Emerging infections. Biomedical Research Reports. Academic Press, New York.

Melnick, J.L., 1994. Live attenuated poliovirus vaccines. In: Plotkin, S.A., Mortimer, E.A. (Eds.), Vaccines. Saunders, Philadelphia, pp. 155–161.

Melnick, J.L., Ledinko, N., 1953. Development of neutralizing antibodies against the three types of poliomyelitis virus during an epidemic period; the ratio of inapparent infection to clinical poliomyelitis. Am. J. Hyg. 58, 207.

Miller, E., Gay, N., 1997. Effect of age on outcome and epidemiology of infectious diseases. Biologicals 25, 137–142.

Nathanson, N., Martin, J.R., 1979. Epidemiology of poliomyelitis—enigmas surrounding its appearance, epidemicity, and disappearance. Am. J. Epidemiol. 110 (6), 672–692.

Nielsen, N.M., Aaby, P., Wohlfahrt, J., Pedersen, J.B., Melbye, M., Molbak, K., 2001. Intensive exposure as a risk factor for severe polio: a study of multiple family cases. Scand. J. Infect. Dis. 33 (4), 301–305.

Paul, J.R., 1971. A History of Poliomyelitis. Yale University Press, New Haven.

Ranta, J., Hovi, T., Arjas, E., 2001. Poliovirus surveillance by examining sewage water specimens: studies on detection probability using simulation models. Risk Anal. 21 (6), 1087–1096.

Roberts, L., 2004. Polio: health workers scramble to contain African epidemic. Science 305, 24–25.

Sabin, A.B., 1981. Paralytic poliomyelitis—old dogmas and new perspectives. Rev. Infect. Dis. 3 (3), 543–564.

Schenzle, D., 1984. An age-structured model of pre- and post-vaccination measles transmission. IMA J. Math. Appl. Med. Biol. 1, 169–191.

Scherer, A., McLean, A., 2002. Mathematical models of vaccination. Br. Med. Bull. 62, 187–199.

Sutter, R.W., Cochi, S.L., Melnick, J.L., 1999. Live attenuated poliovirus vaccines. In: Plotkin, S.A., Orenstein, W.A. (Eds.), Vaccines. Saunders, Philadelphia, pp. 364–403.

Thomas, M.D., Robbins, F.C., 1997. Polio. University of Rochester Press, Rochester, NY.

Van den Driessche, P., Watmough, J., 2002. Reproduction numbers and sub-threshold endemic equilibria for compartmental models of disease transmission. Math. Biosci. 180, 29–48.

Watts, D.J., Strogatz, S.H., 1998. Collective dynamics of 'small-world' network. Nature 393, 440–442.

World Health Assembly, 1988. Global Eradication of Poliomyelitis by the Year 2000. World Health Organization, Geneva.

WHO, 1993. Immunological Basis for Immunization, Module 6: Poliomyelitis. http://www.who.int/vaccines-documents/DocsPDF-IBI-e/mod6_e.pdf

WHO, 2003. Polio eradication: 7 countries and US$210 million to go, Geneva. WHO 81 (9), 629–697.